Article

Not peer-reviewed version

Two Novel Avastrovirus Species Expand the Host Range of Astroviridae to Psittaciformes

K. Jenns *, John-Sebastian Eden, Annabelle Olsson, David Phalen

Posted Date: 3 February 2025

doi: 10.20944/preprints202502.0024.v1

Keywords: astrovirus; virus discovery; metatranscriptomics; parrots; Psittaciformes

Article

Two Novel Avastrovirus Species Expand the Host Range of Astroviridae to Psittaciformes

K. Jenns [1,2,*], John-Sebastian Eden [1,2], Annabelle Olsson [3] and David Phalen [3]

[1] Centre for Virus Research, Westmead Institute for Medical Research, Westmead, New South Wales, Australia

[2] Sydney Institute for Infectious Diseases, School of Medical Sciences, The University of Sydney, Sydney, New South Wales, Australia

[3] Sydney School of Veterinary Science, The University of Sydney, Camden, New South Wales, Australia

* Correspondence: k9.jenns@sydney.edu.au

Abstract: Metatranscriptomics has recently expanded the species richness and host range of the *Avastrovirus* genus, quadrupling the number of avian orders known to host them in less than a decade. Despite this growing awareness of astrovirus presence in wild birds, limited attention has been paid to these viruses in the context of disease in Australian avifauna. Here we used unbiased RNA sequencing of intestinal samples from a galah (*Eolophus roseicapilla*) and an Australian king parrot (*Alisterus scapularis*) with a chronic diarrhoeal and wasting disease to detect the entire genomes of two novel astrovirus species, *Avastrovirus eolorosei* (PQ893528) and *Avastrovirus aliscap* (PQ893527). The phylogenetic positions of these viruses highlight the importance of current and future metatranscriptomic virus screening in investigations of avian host landscapes beyond Galloanserae. This is also the first documentation of avastrovirus infections in Psittaciformes and the first to report their potential role as disease agents in them.

Keywords: astrovirus; virus discovery; metatranscriptomics; parrots; Psittaciformes

1. Introduction

Astroviruses are positive sense nonenveloped RNA viruses. They have 6.1-7.3 kb long genomes with three open-reading frames that encode a serine protease (ORF1a), RNA-dependent RNA polymerase (RdRp, ORF1b), and capsid precursor protein (CaP, ORF2). There are currently two genera within the Astroviridae family, *Mamastrovirus* from mammalian hosts, and *Avastrovirus* from avian hosts, with increasing evidence for a clade within or near this genus of viruses that infect frogs and reptiles [1,2]. The first described Avastroviruses were predominately associated with poultry species and their wild counterparts [3]. It is now known that avastroviruses also infect members of the families Charadriiformes [4,5], Columbiformes [6,7], and Passeriformes [8,9]. Additionally, individual cases of novel avastroviruses have also been identified in an Adélie penguin (*Pygoscelis adeliae*, Sphenisciformes) [10], a broad-billed prion (*Pachyptila vittata*, Procellariiformes) [11], and a red-crowned crane (*Grus japonensis*, Gruiformes) [9]. Since these discoveries, it has been suggested that there are likely many novel avastrovirus species circulating in wild and urban avifauna that are yet to be described [5,12].

In intensively raised poultry, avastroviruses cause enteritis in turkeys, nephritis in chickens and hepatitis in ducks [13–17]. In contrast, most avastroviruses that were detected in wild birds were detected in birds that were apparently healthy or had died from unknown causes, the exception being an astrovirus detected in brain tissues from several species of Australian passerines exhibiting neurological signs [12].

 doi:10.20944/preprints202502.0024.v1

In this report, we describe the complete sequences of two novel avastroviruses, one from a wild recently fledged galah (*Eolophus roseicapilla*) and a second from a wild recently fledged Australian king parrot (*Alisterus scapularis*). Both parrots were suffering from a previously described syndrome characterized by chronic diarrheal disease resulting in severe weight loss and ultimately death. The syndrome occurs in galahs, Australian king parrots, long-billed corellas (*Cacatua tenuirostris*), and sulfur-crested cockatoos (*Cacatua galerita*) [18–21]. The cause of this disease may be multifactorial with birds being typically concurrently infected with one or more of the following: the immunosuppressive psittacine beak and feather disease virus, a yeast (*Macrorhabudus ornithogaster*), a single-celled parasite (*Spironucleus* species) and various bacterial pathogens. Additionally, on the two occasions where electron microscopy has been used to examine the droppings of affected birds, one or more viruses with a morphology consistent with that of an astrovirus have always been identified [18,19].

2. Materials and Methods

2.1. Case Histories and Necropsy

Five recently fledged sub adult galahs (*Eolophus roseicapilla*) were submitted to the Avian Reptile and Exotic Pet Hospital of the University of Sydney (Tharawal country*) in January 2021. All were rescued from the same location in the Macarthur region of NSW, Australia. All individuals had similar signs including severe pectoral muscle atrophy and fetid diarrhoea that was liquid and contained gas. All birds were euthanized following induction with isoflurane gas (Dechra Veterinary Products) in oxygen and then given pentobarbitone (Lethabarb) diluted 1:4 with saline slowly IV to effect. A complete necropsy was performed on one individual and the entire gastrointestinal tract was aseptically resected and stored at -80 ºC until further processing.

The recently fledged Australian king parrot included in this study was one of 40 Australian king parrots (*Alisterus scapularis*) that presented to the Boongarry Veterinary Services, Cairns (Gimuy, Yidinji country*) during the summer of 2021. The bird was exhibiting signs of weight loss and diarrhoea identical to those seen in the galahs. It was euthanised because of its poor prognosis. The small and large intestines were aseptically removed and stored at -20 ºC until further processing.

2.2. Tissue Processing, RNA Extraction, and Library Preparation

Samples from each case were handled, processed, and analysed separately. Tissues were defrosted on dry ice and a 5 mm^3 cross section of the small intestine was placed in 2 mL of DNA/RNA Shield (Zymo Research). These were homogenised for two minutes using a TissueRuptor (QIAGEN) then centrifuged at 8,000 RCF. Clarified homogenates were taken forward for total nucleic acid extraction with ZymoBIOMICS DNA/RNA Miniprep Kit. We prepared RNA libraries for next generation sequencing using an established workflow –RAPID*prep* [22]. Briefly, samples underwent ezDNase treatment (Invitrogen), FastSelect HMR & Bacteria & globin mRNA removal (QIAGEN), single-strand cDNA synthesis with SuperScript™ IV VILO™ Master Mix (Invitrogen), and second-strand cDNA synthesis with Sequenase (ThermoFisher). ds-cDNA was cleaned up with Mag-Bind® Total Pure NGS (Omega Bio-tek). Library preparation included tagmentation and indexation using Nextera XT DNA Library Prep Kit with unique dual indexes (Illumina).

2.3. Next Generation Sequencing and Metatranscriptomic Analysis

To ensure accurate pooling, we sequenced libraries together on a single iSeq (Illumina) run and used percent passing filter as a quality check to calculate appropriate input volumes for downstream sequencing. The resulting library pool was sequenced on a NovaSeq X platform (Illumina) by the Australian Genomic Research Facility (Melbourne/Naarm, Wurundjeri country*) using a 10B (300 cycle) flow cell. Each library was sequenced to a minimum read depth of 40 million paired reads. Raw reads were processed through an in-house metatranscriptomic analysis pipeline. Briefly, we performed host removal of the galah library using an index of the galah reference genome

 doi:10.20944/preprints202502.0024.v1

(GCA_013397615) Bowtie2 v2.4.4 [23] and samtools v1.9 [24]. There is currently no genome available for the Australian king parrot, so we built a Bowtie2 index from the reference genome of the Alexandrine parakeet (*Psittacula eupatria*, GCA_031762335) and applied the same approach. Host-filtered reads were trimmed and deduplicated using fastp v0.22.0 [25] and quality filtered to remove low-complexity sequences with prinseq v0.20.4 [26]. We then sorted and selected non-ribosomal reads using sortmeRNA v4.3.3 [27]. To ensure removal of any human DNA contamination, non-rRNA reads were filtered using a two-step approach: i) k-mer matching against a human pan-genome database with Kraken2 v2.0.8-beta [28,29] and ii) alignment against the telmore-2-telomere reference genome (GCF_009914755) and human leukocyte antigen sequences (https://github.com/ANHIG/IMGTHLA/) using Bowtie2 [23].

These reads were *de novo* assembled using MEGAHIT v1.1.3 [30] and we remapped the filtered reads back to the resulting contigs using Bowtie2 [23] to extract unassembled reads. Kallisto v0.46.0 was used to establish contig abundance [31]. We then aligned the contigs and unassembled reads to the NCBI nucleotide database (nt, downloaded 2023-06-27) using BLAST+ v.2.11.0 [32] and to the NCBI non-redundant protein database (nr, downloaded 2023-06-27) using Diamond v0.9.32 [33].

2.4. Novel Astrovirus Characterisation

We retrieved a complete and near complete genome of astroviruses with low sequence identity to known sequences available in our nt and nr databases from the galah and king parrot libraries, respectively. To retrieve more coverage of the king parrot-associated astrovirus genome, we determined relevant genomic positions of available contigs in GeneiousPrime using known avastrovirus sequences as reference and remapped the host filtered non-rRNA reads to this draft genome using bbmap v37.98 [34]. We annotated both novel astrovirus genomes with canonical ORFs of the virus family and with protein domains according to conserved domain database search from NCBI [35,36] and HMMER [37,38].

2.5. Phylogenetic Analyses

We aligned the translated protein sequence of the RdRp domain of our novel viruses with all known astrovirus sequences available on GenBank (accessed 2024-08-15) using the L-INS-i algorithm in MAFFT v7.490 [39]. The alignment was trimmed manually and sites with >80% gaps were stripped. The alignment was modified to display only representative astrovirus species with ≤95% amino acid identity in this domain to other available sequences. This alignment was used to generate a maximum likelihood phylogeny in IQ-TREE 2 v2.2.2 with 1000 bootstrap branch supports and the best fit substitution model selection [40]. This process was repeated using translated sequences from ORF2 of the CaP domain. A representative phylogeny including the same accessions as the RdRp was constructed, as well as a more extensive phylogeny to include richer diversity of ANV strains and passerine astroviruses.

2.6. Predictive Analyses

To investigate patterns of asparagine-linked glycosylation (N-glycosylation) on the capsid protein of KPAstV and GAstV, we queried amino acid sequences of the entire ORF2 translation in the NetNGlyc-1.0 server prediction tool [41]. This analysis was expanded to include all sequences utilised in the expanded CaP domain phylogeny. These complete ORF2 translations were aligned using the E-LNS-i algorithm in MAFFT and the resulting alignment was trimmed manually. Predicted N-glycosylation sites with significant NetNGlyc results (>0.5) were annotated on each sequence of the alignment. The alignment was also annotated with the locations of the capsid precursor and spike domains of Turkey astrovirus 2 (TAstV-2), previously determined with x-ray diffraction [42].

To determine the predicted 3D structure of the KPAstV and GAstV spike proteins, we performed in silico protein homology modelling using SWISS-MODEL [43,44]. Protein translations of ORF2

 doi:10.20944/preprints202502.0024.v1

were used as queries and models were built using template crystal structure of TAstV-2 (SMTL ID 3ts3.1). This analysis was then repeated for sequences that captured representative diversity of the genus to contextualise the findings of the novel viruses.

3. Results

This section may be divided by subheadings. It should provide a concise and precise description of the experimental results, their interpretation, as well as the experimental conclusions that can be drawn.

3.1. Necropsy Findings

The galah and king parrot were found to have loops of small bowel that were thin-walled to the point of being nearly transparent that contained a liquid bile-stained content. The most significant microscopic lesions were a diffuse severe chronic lymphoplasmacytic enteritis with villus blunting and fusion and hyperplasia of the crypt epithelium of the duodenum and proximal jejunum. Renal, hepatic and brain lesions were not observed.

3.2. Metatranscriptomic Libraries

Following quality trimming, host removal, and rRNA depletion, the galah and king parrot libraries contained 5,630,332 (4.67% total) and 3,926,189 (9.97% total) read pairs, respectively. We recovered a genome-length astrovirus-like contig (6,894 bp) from the galah library. Over 50% of the quality filtered galah library read pairs mapped to this sequence, with an abundance of 6.7e04 TPM. We assembled three contigs into a genome-length scaffold (6,825 bp) from the king parrot library and finalised this draft genome through read mapping. The completed genome had >2% of the quality filtered reads mapped to it. Based on the hosts in which they were identified, we name these novel viruses *Avastrovirus eolorosei* (GAstV, from the galah) and *Avastrovirus aliscap* (KPAstV, from the king parrot) and their sequences have been deposited to GenBank under the accessions PQ893528 and PQ893527, respectively.

Beak-and-feather virus (BFDV) was identified at lower abundance (<0.1% of filtered reads) in both libraries.

3.3. Genome Annotation and Alignments

The genome architecture of both viruses is typical of astroviruses (Figure 1), including the heptameric slippery ribosomal frameshift motif "AAAAAAC" between ORF1a and ORF1b and the RNA synthesis promoter upstream of ORF2 proposed by Mendez and Arias in 2007. Both viruses differ to this sequence by only four 5′ end nucleotides each (Figure 1). KPAstV is the first documented member of Astroviridae to contain only four nucleotides in the 3′ variable region directly upstream of the ORF2 start codon, which typically contains five to eight bases.

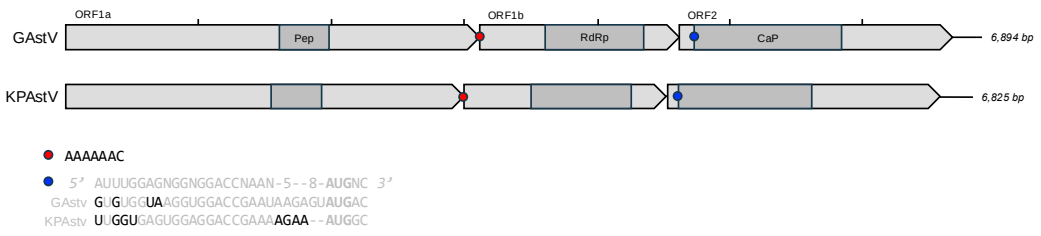

Figure 1. Genome architecture of GAstV and KPAstV. Both viruses contain the canonical three open reading frame structure of astroviruses shown in light grey arrows, with the ribosomal slippage heptamer indicated between ORF1a and ORF1b (red circle). The blue circle highlights an alignment of the proposed subgenomic RNA synthesis promoter sequence with GAstV (second row) then KPAstV (third row). Here, the ORF2 start codon is in bold and deviations from the proposed sequence are shown in black letters, rather than grey.

 doi:10.20944/preprints202502.0024.v1

Conserved protein domains are depicted in dark grey include the trypsin-like peptidase (pfam13365), Astroviridae RNA-dependent RNA polymerase (cd23172), and Astrovirus capsid protein precursor (cl46880).

The highly conserved RdRp domains of GAstV and KPAstV have low protein identity (<65.2 and <83.5%, respectively) with publicly available astrovirus sequences, as of in August 2024 (Table 1). Similarly, a masked alignment of the capsid precursor domain revealed only 47.3 and 74.2% identity among closest relatives of these viruses. KPAstV shares maximum identity across both domains and the complete translated sequence of ORF2 with Avian astrovirus strain pigeon/China/20/2014 (MF768270). GAstV holds greatest identity with three different viruses across the three alignments, likely due to its deep divergence. Both viruses exceed the minimum requirements of species demarcation criteria currently outlined by the International Committee for the Taxonomy of Viruses, having distinct hosts from their phylogenetic neighbours and <75.0% amino acid identity with any other avastrovirus in the complete ORF2 translation alignment, hence we suggest they both be considered novel *Avastrovirus* species.

Table 1. Mean percent identity of GAstV and KPAstV across different protein alignments. Protein identity was provided by manually trimmed MAFFT alignments of each region. Domain-based alignments had sites containing greater than 80% gaps stripped. The mean was calculated across consistent phylogenetic clades defined in Figure 2 and the maximum identity score and reference accession is provided for novel each virus and alignment.

Alignment	Mean±SD %ID	GAstV	KPAstV
RdRp domain	Clade 1 (poultry)	61.68±1.59	58.10±2.06
	Clade 2 (diverse)	61.68±3.13	71.41±9.26
	Clade 3 (herp)	51.37±5.14	48.82±3.14
	Clade 4 (passerine)	59.61±1.83	55.09±1.66
	Outgroup (marmot)	46.36±1.52	45.45±0.23
	Maximum ID	*65.2*[a]	*83.53*[b]
Capsid precursor domain	Clade 1 (poultry)	39.30±2.99	38.18±1.94
	Clade 2 (diverse)	46.11±1.62	37.93±8.22
	Clade 3 (herp)	31.33±1.83	35.28±2.28
	Clade 4 (passerine)	36.82±1.86	44.76±1.83
	Outgroup (marmot)	27.09±1.03	25.46±2.18
	Maximum ID	*47.28*[c]	*74.22*[b]
Complete ORF2	Clade 1 (poultry)	28.81±3.71	24.09±4.03
	Clade 2 (diverse)	22.79±1.00	46.26±08.28
	Clade 3 (herp)	19.39±5.66	19.44±7.47
	Clade 4 (passerine)	19.78±3.08	18.29±3.54
	Outgroup (marmot)	7.75±0.48	6.71±0.46
	Maximum ID	*35.17*[d]	*58.57*[b]

[a]MT138004, [b]MF768270, [c]MW588064, [d]MT894397.

3.4. Phylogenetic Analyses

Both KPAstV and GAstV reside within the broader diversity of the *Avastrovirus* genus (Figure 2). The discovery of these viruses in Psittaciformes expands the number of avian orders known to host astroviruses to eight. Phylogenetic analyses of both conserved domains revealed that KPAstV clusters within Clade 2, among ANV and avastroviruses from a wide range of unrelated avian hosts (Figure 2, Supplementary Figure S1). The RdRp of GAstV, on the other hand, lies outside the known diversity of avian-hosted avastroviruses but its CaP clusters within poultry-associated avastroviruses of Clade 1 (Figure 2). There was no evidence to suggest recombination in KPAstV. The relative novelty of the GAstV RdRp domain may be explained by recombination but, without more closely related strains for comparison, this is difficult to assess.

 doi:10.20944/preprints202502.0024.v1

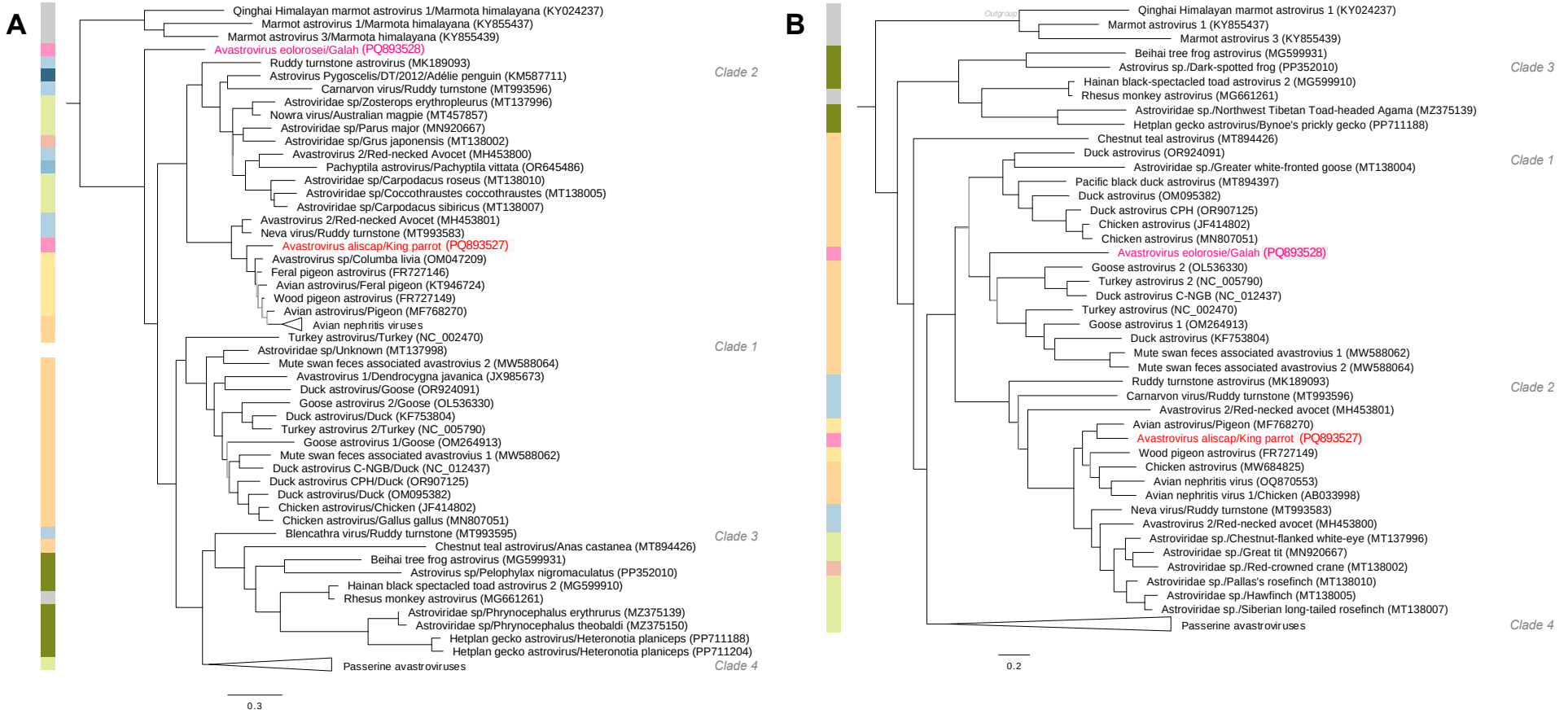

Figure 2. Maximum likelihood phylogenies of avian astroviruses. **(A)** The RdRp tree was generated from an alignment of 250 amino acids of the Astroviridae RdRp domain (cd23172). **(B)** The CaP tree was generated from an alignment of 377 amino acids of the astrovirus capsid precursor protein domain (cl46880). Phylogenies were constructed in IQ-TREE 2 [40] using ModelFinder with 1000 Ultrafast bootstrap supports and are rooted on the marmot astrovirus outgroup. Nodes with fewer than 70% support are drawn in pale grey. GAstV and KPAstV are shown in pink and red text, respectively. Phylogenetic clades that are consistent across both domains are shaded with grey boxes. Host association for each sequence is summarised in panels adjacent to each tree with colours representing avian orders and non-avian classes: Reptilia and Amphibia (dark green), Mammalia (grey), Anseriformes and Galliformes (orange), Charadriiformes (pale blue), Columbiformes (yellow), Gruiformes (pale red), Passeriformes (pale green), Procellariiformes (blue), Psitticiformes (pink) and Sphenisciformes (dark blue).

 doi:10.20944/preprints202502.0024.v1

3.5. Predicitive Analyses

To compare the biology, evolution, and potential pathogenesis of these viruses, we examined the capsid and spike domains of ORF2 using structural and glycosylation prediction analyses. All clades of Avastrovirus show more confident, numerous, and conserved predicted N-glycosylation (GlyN) patterns in the conserved CaP domain than in the spike domain (Supplementary Figure S2). The region with greatest N-glycosylation occurs in the CaP domain of Clade IV, the passerine astroviruses, followed by Clade III. KPAstV has two CaP-associated GlyNs but none in the spike domain, whereas GAstV has one in each. The first GlyN of KPAstV – N220 Y221 T222 G223 – is identical to that of Neva virus (MT993583). Its second – N336 D337 T338 S339 – has 75% identity to the Feral pigeon astrovirus (FR727146), N344 D345 T346 K347. The CaP GlyN of GAstV – N81 R82 S83 W84 – has 75% identity with three crow-associated astroviruses (KT946719-20, MW385413). There is no single conserved GlyN in the spike domain of ANV species (n=15) nor across the canonical poultry pathogens. In contrast a highly conserved GlyN is present in the CaP domain at sites 319-322 of the ORF2 alignment across all four major clades of Avastrovirus – in nearly all ANV strains, a wood pigeon astrovirus, a red-necked avocet astrovirus, mute swan faeces-associated astroviruses, several passerine astroviruses and the Hetplan gecko astrovirus.

Predicted protein models based on the experimentally derived crystal structure of TAstV-2 capsid spike [42] reveal two distinct structures within *Avastrovirus* Clades I and II (Figure 3). Significant 3-dimensional homology with the homodimer configuration of TAstV-2, with centrally aligned N- and C-termini, asymmetrical apical bulges, and surface glycosylation, is observed in other representatives from Clade I (Figure 3L,M), and in three strains of ANV (Figure 3H–J). It is also the predicted structure of Neva virus and a feral pigeon Avian astrovirus from Clade II (Figure 3C,F). These are outliers among other members of the clade, where KPAstV, two pigeon astroviruses and two red-necked avocet astroviruses share a distinct structure of that features symmetrically distributed dimers, surface hairpins, weaker central alignment of the termini, and little to no surface glycosylation (Figure 3A,B,D,E,G,N). Sequences that aligned with the TAstV-2 structure had significantly higher amino acid percentage identity with TAstV-2, Global Model Quality Estimates (GMQE), and QMEANDisCo global scores than sequences with KPAstV-like models (Supplementary Table S1). No templates were found for the C-terminal region of the GAstV ORF2 protein, nor of Astroviridae sp. (Clade II, MT138010), Hetplan gecko astrovirus (Clade III, PP711188), and Passerine astrovirus 1 (Clade IV, MK096773), so were not included further in the analysis. Together, these results show that there was no apparent conserved spike structure within the KPAstV-related avastrovirus clade.

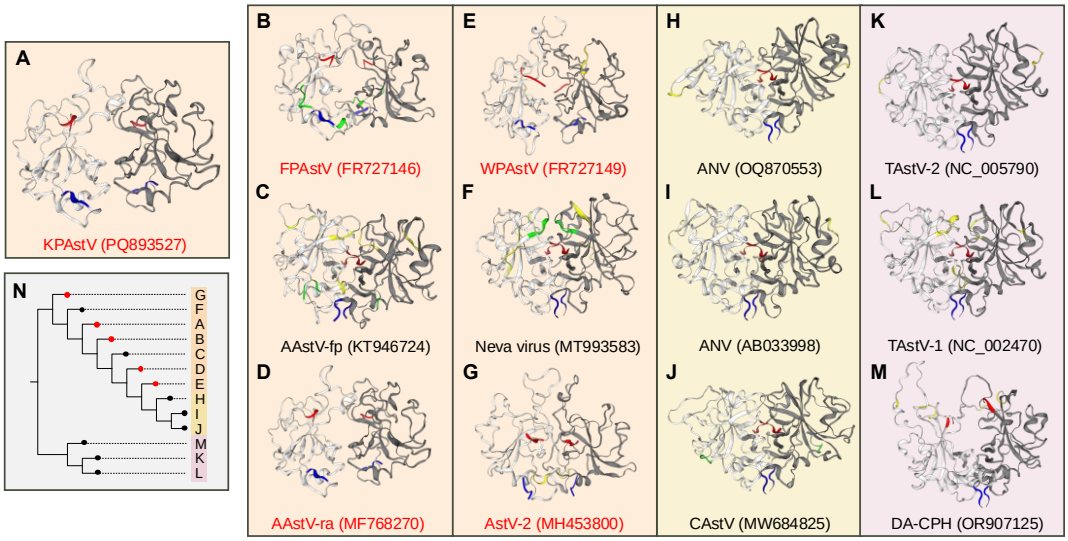

 doi:10.20944/preprints202502.0024.v1

Figure 3. Predicted homo-dimeric protein structures of Avastrovirus capsid spike domains. C-terminus regions of translated ORF2 beyond the conserved capsid precursor protein domain were searched against the database of protein structure templates in SWISS-MODEL. Models were built where homology to the Turkey astrovirus 2 capsid spike 3ts3.1.A template [42] was found in **(A)** *Avastrovirus aliscap* (KPAstV), king parrot, **(B)** *Avian astrovirus* (AAstV-ra), pigeon, **(C)** *Wood pigeon astrovirus* (WPAstV), wood pigeon, **(D)** *Feral pigeon astrovirus* (FPAstV), feral pigeon, **(E)** *Neva virus*, ruddy turnstone, **(F)** *Avastrovirus 2* (AstV-2), red-necked avocet, **(G)** *Avian astrovirus* (AAstV-fp), feral pigeon, **(H)** *Avian nephritis virus* (ANV), chicken, **(I)** *Avian nephritis virus* (ANV), chicken, **(J)** *Chicken astrovirus* (CAstV), chicken, **(K)** *Turkey astrovirus 2* (TAstV-2), turkey, **(L)** *Turkey astrovirus 1* (TAstV-1), and **(M)** *Duck astrovirus CPH* (DA-CPH), duck. **(N)** The relative phylogenetic relationships between the viruses analysed in A-M as a cladogram. Chains of each homodimer are drawn in white and grey, with N- and C-termini drawn in blue and red, respectively. Predicted N-glycosylation tetrapeptides are drawn in yellow (N-Glyc result 0.5-0.65) and green (N-Glyc result 0.65-0.75). Background colours (panels A-M) and tip label highlighting (panel N) correspond to Clade I (pink), non-ANV Clade II (orange), and ANV Clade II (yellow) from Figure 2. Dimeric structures similar to KPAstV are written (panels A-M) and depicted with tip circles (panel N) in red, while those similar to the crystal structure of TAstV-2 are labelled in black.

4. Discussion

Our use of unbiased metatranscriptomics to identify viruses suspected to be associated with the pathogenesis of a wasting disease in several species of Australian parrots identified two highly abundant novel avastroviruses in the digestive tract of two species of parrots with this syndrome. These findings are significant because they contribute to the understanding of *Avastrovirus* evolution by expanding the diversity and host range of the genus, providing the first and second astroviruses infecting psittacine birds. It also provides preliminary insight into the pathogenesis of a significant wildlife disease.

The genomic architecture of GAstV and KPAstV aligns with other avastroviruses, placing them confidently within the genus (Figure 1). According to ICTV guidelines, low identities of their ORF2 proteins with other sequences of avastroviruses suggest that they are novel species (Table 1). Our phylogenetic analyses revealed that GAstV is more distantly related to other avian-hosted avastroviruses than KPAstV. The deep divergence of the RdRp in GAstV suggests that range of genetic diversity in avastroviruses is greater than previously defined. Furthermore, the discrepancy in the RdRp and CaP tree topologies could be evidence of ancient recombination events amongst this unexplored diversity. It is not uncommon to observe recombination among astroviruses. Recombination is well-documented in avian nephritis virus strains [45,46] and cross-family gene exchange between astro-hepe-like viruses is increasingly being demonstrated several vertebrate hosts, including carnivorous birds [47,48]. KPAstV adds another layer of host complexity to its surrounding diversity which is already extremely host-rich compared to the poultry- and passerine-specific clades (Figure 2, Supplementary Figure S1). Unlike GAstV, KPAstV and the members of its clade are phylogenetically stable across the two conserved domains. The strength of this conclusion will be enhanced when CaP sequence data for the Adélie penguin [10] and broad-billed prion [11] become available. The relatives of KPAstV are pigeon-associated avastroviruses and ANV, which are mostly pathogenic [6,7,49], and ruddy turnstone astroviruses, which are not known to cause disease [5]. Our phylogenies also demonstrate that avastroviruses are present in birds with diverse breeding and feeding behaviours, from transcontinental migratory shorebirds to highly localised wild parrots to urban feral pigeons to farmed poultry. The recent discoveries of avastro-like viruses in lizards and geckos further highlights the expanding genetic diversity of this genus (Figure 2) [2,50]. Hence, given the deep divergence of the viruses described in this study, despite having only investigated two individuals, we concur with Wille et al. 2018 that the diversity of avastroviruses, revealed by few studies in wild birds, points to a much larger reservoir of unidentified enzootic viruses residing in avifauna.

The origins of KPAstV and GAstV are unclear. Based on findings in other birds, avastroviruses can demonstrate either co-evolution in host families or cross-species transmission between more

 doi:10.20944/preprints202502.0024.v1

unrelated hosts. For example, ANV in chickens and turkey astroviruses, which are equally divergent from one another as KPAstV and GAstV, are yet specialised for two phasianid species (Table 1, Figure 2) [51]. Studies in ruddy turnstones, on the other hand, have uncovered similarly divergent astroviruses (e.g., Carnarvon virus, Blencathra virus, and Neva virus) within the same population of a single host species (Figure 2) [5]. Conversely, KPAstV or GAstV may be enzootic astroviruses of other unknown wild bird species that cohabitate or interact with these parrots and repeated cross-species transmission events lead to disease development in the psittacine hosts. This has been observed in the transmission of ANV from chickens to pigeons [6], of TAstV-2 from turkeys to guinea fowl [52], and of unclassified avian astroviruses between wild waterfowl [53] and passerines [9]. Given the novelty of the viruses we describe, especially GAstV, host-virus dynamics can only be resolved through richer metatranscriptomic surveys of Australian avifauna that sample healthy and diseased populations of cohabitating wild species.

N-linked glycosylation of viral proteins is known to enhance infectivity, immune evasion, and host specificity in other RNA viruses, including avian influenza viruses and coronaviruses, and avian infectious bronchitis virus [54–57]. The importance of N-linked glycosylation of the capsid protein in avian astroviruses has not been established. However, maturation and protein cleavage of human astrovirus capsids is well documented [58–60] but this has only been explored experimentally once in a single *Avastrovirus*, TAstV-2 [42]. We compared N-glycosylation sites of the ORF2 domains in an effort to determine patterns of host specificity and pathogenicity. To our knowledge, this is the first comparative analysis of N-glycosylation patterns in ORF2 across the *Avastrovirus* genus (Supplementary Figure S2). We detected two well-supported N-glycosylation site predictions in the capsid precursor protein of KPAstV which were comparable to sites in other Clade II viruses. In contrast, the N-glycosylation pattern of GAstV lacked resemblance to any other *Avastrovirus* clade. While some trends exist in the glycosylation of the capsid precursor domain in Clades III and IV, there was little evidence to support any conservation of spike protein glycosylation patterns. Given the significance of N-glycosylation in other RNA viruses, we suggest that future research on capsid and spike proteins could improve pathogen identification as more avian and mammalian astroviruses are uncovered.

Predicted spike protein models provide insights into the host specificity and evolution of Clade I and II avastroviruses. The crystal structure of TAstV-2 revealed that it had only distant similarities with the spikes of human astroviruses, and suggested its unique structure was associated with its avian host specificity [42]. Our results confirm the prediction of homologous protein architectures within the genus despite low (<30%) protein identity among avastrovirus spike proteins (Supplementary Table S1). Two distinct structures emerged from our analysis, distinguishing poultry-borne Clade I astroviruses and ANV strains from wild bird-borne Clade II astroviruses, with two exceptions in Neva virus and fpAAstV (Figure 3). This may indicate either convergent evolution or an ancestral trait of phasianid-specific spike structures. The strength of our predictions is limited by access to only one experimentally derived protein crystal structure, despite the agricultural significance of the genus [42]. Experimental determination of the ANV spike protein, for example, being phylogenetically distinct from TAstV-2 and a widely accessible model for avastrovirus infections, will enhance our understanding of its role in host cell interactions and virulence. This work highlights the value of analysing the spike protein structure to assess the long term evolution of avastroviruses across the broad range of hosts they infect.

Astroviruses can cause acute or chronic diarrhoea and enteritis, as well as disease in other systems. Astroviruses infections are typically acute and self-limiting [13,61,62]. In birds and mammals, they infect mature enterocytes at the villous tips of the small intestine, leading to villous atrophy and epithelial damage. This disruption of absorptive function results in malabsorption and osmotic diarrhoea. Concurrently, barrier dysfunction and immune activation induce mild inflammation which collectively aggravate the diarrhoea and enteritis. The severe chronic lymphoplasmacytic enteritis and blunting and fusion of the villi in our two cases are consistent with histopathology observed in acute astrovirus infections in turkey, chickens, geese, ducks and pigeons

 doi:10.20944/preprints202502.0024.v1

[6,49,51,63–66] and hence may have been an important contributor to the diarrhoea and weight loss seen in these birds and other birds with this syndrome. The chronic disease progression in the two case individuals is similar to what has been observed in immunosuppressed humans [61,67]. Concurrent infections with the immunosuppressive psittacine beak and feather disease virus were observed in the two birds in this study and has been documented in other birds with this syndrome. Hence, co-infection with beak-and-feather disease virus may prove to be an important factor in the aetiology of this disease and the apparent chronic astrovirus infection that we observed in the two birds we studied.

In this study, we have reason to believe that the astroviruses that we discovered were enterotropic because they were found in samples of the small intestines. Other studies on the diversity of avastroviruses in wild birds have screened birds using cloacal swabs [4,5,8,9]. Cloacal swabs are an easy and minimally invasive tool for screening for virus shedding. However, cloacal swabs have a limitation in that a virus detected in them could originate from either the digestive tract or the kidney, given that the contents of the cloaca are composed of faeces and urine [68]. Future studies that screen for avastroviruses in dead birds should collect samples from both intestines and the kidney where it is possible and this may help to determine if capsid proteins contain tissue specific sequences.

The two parrots in this study where shedding large concentrations of Avastrovirus. This means that these parrots and other psittacine birds with this syndrome should be strictly quarantined when hospitalised or housed in rehabilitation facilities so as not to infect other birds housed in these facilities. The disease presentation and progression in our case studies is very similar to those of galahs and a sulfur-crested cockatoo from Perth [18], galahs and sulfur-crested cockatoos from Victoria in 1991 [19], king parrots from the south-eastern states of Australia through 1984-2000 [20], and galahs in south-east Queensland from 2002-2012 [21]. Together, given that the king parrot in our study was from north Queensland and the galah from NSW, this indicates the potential for continent-wide distribution of the aetiological agent or agents involved in this complex disease. Additionally, Australia contains one of the largest groups of endemic parrot species and consequently, there are considerable biosecurity concerns that importation of exotic parrots either for pets or for avicultural may bring in pathogens that are not present in Australia. The 2020 Australian Government report on psittacine bird imports deemed astroviruses as “not of significance” [69]. Our work suggests that novel avastroviruses could also be circulating in psittacine birds originating from outside of Australia. Therefore, psittacine birds being imported from other countries into Australia should be tested for and be free of avastroviruses before they are allowed to enter the country.

Supplementary Materials: The following supporting information can be downloaded at the website of this paper posted on Preprints.org, Figure S1: Expanded maximum likelihood phylogeny of the RNA dependent RNA polymerase of avian astroviruses; Figure S2: Predicted N-glycosylation in *Avastrovirus* ORF2 translated protein; Table S1: SWISS-MODEL results for *Avastrovirus* spike proteins.

Author Contributions: Conceptualization, K.J. and D.P.; methodology, K.J., D.P., A.O., and J.E.; formal analysis, K.J. and D.P.; investigation, D.P. and A.O.; data curation, K.J.; writing—original draft preparation, K.J.; writing—review and editing, D.P. and J.E.; visualization, K.J.; supervision, D.P. and J.E.; project administration, D.P. and J.E.; funding acquisition, D.P. and J.E. All authors have read and agreed to the published version of the manuscript.

Funding: This research was funded in part by a grant from WIRES New South Wales, grant number R3112 RG346_PJ

Data Availability Statement: Quality- and host-filtered paired reads have been deposited in the Sequence Read Archive (SRA) under the accession numbers SRR31990207-8.

Acknowledgments: *Place names: Out of respect for the diverse nations of traditional custodians on the Australian continent, we utilise Indigenous place and country names where possible. The authors of this paper acknowledge Elders, past and present, of the lands on which this study was prepared – the Gadigal,

 doi:10.20944/preprints202502.0024.v1

Burramattagal, and Arrente people – and from which samples were retrieved, who have cared for land and waters for time immemorial.

Conflicts of Interest: The authors declare no conflicts of interest.

References

1. Shi, M.; Lin, X.D.; Chen, X.; Tian, J.H.; Chen, L.J.; Li, K.; Wang, W.; Eden, J.S.; Shen, J.J.; Liu, L.; Holmes, E.C. The evolutionary history of vertebrate RNA viruses. *Nature* **2018**, *556*, 197–202.
2. Mahar, J.E.; Wille, M.; Harvey, E.; Moritz, C.C.; Holmes, E.C. The diverse liver viromes of Australian geckos and skinks are dominated by hepaciviruses and picornaviruses and reflect host taxonomy and habitat. *Virus Evol.* **2024**, *10*.
3. King, A.M.; Lefkowitz, E.; Adams, M.J.; Carstens, E.B. *Virus taxonomy: ninth report of the International Committee on Taxonomy of Viruses*, 9th ed.; Elsevier 2011; Volume 9.
4. Wille, M.; Eden, J.S.; Shi, M.; Klaassen, M.; Hurt, A.C.; Holmes, E.C. Virus–virus interactions and host ecology are associated with RNA virome structure in wild birds. *Mol. Ecol.* **2018**, *27*(24), 5263–5278.
5. Wille, M.; Shi, M.; Hurt, A.C.; Klaassen, M.; Holmes, E.C. RNA virome abundance and diversity is associated with host age in a bird species. *Virology* **2021**, *561*, 98–106.
6. Zhao, W.; Zhu, A.L.; Yuan, C.L.; Yu, Y.; Zhu, C.X.; Lan, D.L.; Yang, Z.B.; Cui, L.; Hua, X.G. Detection of astrovirus infection in pigeons (Columbia livia) during an outbreak of diarrhoea. *Avian Pathol.* **2011**, *40*, 361–365.
7. Kofstad, T.; Jonassen, C.M. Screening of feral and wood pigeons for viruses harbouring a conserved mobile viral element: characterization of novel astroviruses and picornaviruses. *PloS One* **2011**, *6*, 25964.
8. Fernández-Correa, I.; Truchado, D.A.; Gomez-Lucia, E.; Doménech, A.; Pérez-Tris, J.; Schmidt-Chanasit, J.; Cadar, D.; Benítez, L. A novel group of avian astroviruses from Neotropical passerine birds broaden the diversity and host range of Astroviridae. *Sci. Rep.* **2019**, *9*, 9513.
9. Shan, T.; Yang, S.; Wang, H.; Wang, H.; Zhang, J.; Gong, G.; Xiao, Y.; Yang, J.; Wang, X.; Lu, J.; Zhao, M. Virome in the cloaca of wild and breeding birds revealed a diversity of significant viruses. *Microbiome* **2022**, *10*, 60.
10. Grimaldi, W.W.; Hall, R.J.; White, D.D.; Wang, J.; Massaro, M.; Tompkins, D.M. First report of a feather loss condition in Adelie penguins (Pygoscelis adeliae) on Ross Island, Antarctica, and a preliminary investigation of its cause. *Emu* **2015**, *115*, 185–189.
11. Grimwood, R.M.; Reyes, E.M.; Cooper, J.; Welch, J.; Taylor, G.; Makan, T.; Lim, L.; Dubrulle, J.; McInnes, K.; Holmes, E.C.; Geoghegan, J.L. From islands to infectomes: host-specific viral diversity among birds across remote islands. *BMC Ecol. Evol.* **2024**, *24*, 84.
12. Chang, W.S.; Eden, J.S.; Hall, J.; Shi, M.; Rose, K.; Holmes, E.C. Metatranscriptomic analysis of virus diversity in urban wild birds with paretic disease. *J. Virol.* **2020**, *94*, 10–1128.
13. Koci, M.D.; Schultz-Cherry, S. Avian astroviruses. *Avian Pathol.* **2002**, *31*, 213–227.
14. Fu, Y.; Pan, M.; Wang, X.; Xu, Y.; Xie, X.; Knowles, N.J.; Yang, H.; Zhang, D. Complete sequence of a duck astrovirus associated with fatal hepatitis in ducklings. *J. Gen. Virol.* **2009**, *90*, 1104–1108.
15. Todd, D.; Smyth, V.J.; Ball, N.W.; Donnelly, B.M.; Wylie, M.; Knowles, N.J.; Adair, B.M. Identification of chicken enterovirus-like viruses, duck hepatitis virus type 2 and duck hepatitis virus type 3 as astroviruses. *Avian Pathol.* **2009**, *38*, 21–29.
16. Pantin-Jackwood, M.J.; Strother, K.O.; Mundt, E.; Zsak, L.; Day, J.M.; Spackman, E. Molecular characterization of avian astroviruses. *Arch. Virol.* **2011**, *156*, 235–244.
17. Janowski, A.B. Beyond the gastrointestinal tract: the emerging and diverse tissue tropisms of astroviruses. *Viruses* **2021**, *13*, 732.
18. Wylie, S.L.; Pass, D.A. Investigations of an enteric infection of cockatoos caused by an enterovirus-like agent. *Aust. Vet. J.* **1989**, *66*, 321–324.
19. McOrist, S.; Madill, D.; Adamson, M.; Philip, C. Viral enteritis in cockatoos (Cacatua s). *Avian Pathol.* **1991**, *20*, 531–539.

 doi:10.20944/preprints202502.0024.v1

20. Philbey, A.W.; Andrew, P.L.; Gestier, A.W.; Reece, R.L.; Arzey, K.E. Spironucleosis in Australian king parrots (Alisterus scapularis). *Aust. Vet. J.* **2002**, *80*, 154–160.
21. Doneley, B. Weight loss syndrome in juvenile free-living galahs (Eolopus roseicapillus). In Proceedings of the Annual Conference of the Australasian Association of Avian Veterinarians and Unusual and Exotic Pet Veterinarians, 9–11 January 2012.
22. Tulloch, R.L.; Kim, K.; Sikazwe, C.; Michie, A.; Burrell, R.; Holmes, E.C.; Dwyer, D.E.; Britton, P.N.; Kok, J.; Eden, J.S. RAPID prep: A Simple, Fast Protocol for RNA Metagenomic Sequencing of Clinical Samples. *Viruses* **2023**, *15*, 1006.
23. Langmead, B.; Salzberg, S.L. Fast gapped-read alignment with Bowtie 2. *Nat. Methods* **2012**, *9*, 357–359.
24. Li, H.; Handsaker, B.; Wysoker, A.; Fennell, T.; Ruan, J.; Homer, N.; Marth, G.; Abecasis, G.; Durbin, R.; 1000 Genome Project Data Processing Subgroup. The sequence alignment/map format and SAMtools. *Bioinformatics* **2009**, *25*, 2078–2079.
25. Chen, S.; Zhou, Y.; Chen, Y.; Gu, J. fastp: an ultra-fast all-in-one FASTQ preprocessor. *Bioinformatics* **2018**, *34*, 884–890.
26. Schmieder, R.; Edwards, R. Fast identification and removal of sequence contamination from genomic and metagenomic datasets. *PloS One* **2011**, *6*, 17288.
27. Kopylova, E.; Noé, L.; Touzet, H. SortMeRNA: fast and accurate filtering of ribosomal RNAs in metatranscriptomic data. *Bioinformatics* **2012**, *28*, 3211–3217.
28. Hall, M.B.; Coin, L.J. Pangenome databases improve host removal and mycobacteria classification from clinical metagenomic data. *GigaScience* **2024**, *13*, 1–10.
29. Wood, D.E.; Lu, J.; Langmead, B. Improved metagenomic analysis with Kraken 2. *Genome Biol.* **2019** *20*, 1–13.
30. Li, D.; Liu, C.M.; Luo, R.; Sadakane, K.; Lam, T.W. MEGAHIT: an ultra-fast single-node solution for large and complex metagenomics assembly via succinct de Bruijn graph. *Bioinformatics* **2015**, *31*, 1674–1676.
31. Bray, N.L.; Pimentel, H.; Melsted, P.; Pachter, L. Near-optimal probabilistic RNA-seq quantification. *Nat. Biotechnol.* **2016**, *34*, 525–527.
32. Camacho, C.; Coulouris, G.; Avagyan, V.; Ma, N.; Papadopoulos, J.; Bealer, K.; Madden, T.L. BLAST+: architecture and applications. *BMC Bioinformatics* **2009**, *10*, 1–9.
33. Buchfink, B.; Reuter, K.; Drost, H.G. Sensitive protein alignments at tree-of-life scale using DIAMOND. *Nat. Methods* **2021**, *18*, 366–368.
34. Bushnell, B. BBMap: a fast, accurate, splice-aware aligner. 2014
35. Marchler-Bauer, A.; Bo, Y.; Han, L.; He, J.; Lanczycki, C.J.; Lu, S.; Chitsaz, F.; Derbyshire, M.K.; Geer, R.C.; Gonzales, N.R.; Gwadz, M. CDD/SPARCLE: functional classification of proteins via subfamily domain architectures. *Nucleic Acids Res.* **2017**, *45*, D200–D203.
36. Wang, J.; Chitsaz, F.; Derbyshire, M.K.; Gonzales, N.R.; Gwadz, M.; Lu, S.; Marchler, G.H.; Song, J.S.; Thanki, N.; Yamashita, R.A.; Yang, M. The conserved domain database in 2023. *Nucleic Acids Res.* **2023**, *51*, D384–D388.
37. Finn, R.D.; Clements, J.; Eddy, S.R. HMMER web server: interactive sequence similarity searching. *Nucleic Acids Res.* **2011**, *39*, W29–W37.
38. Potter, S.C.; Luciani, A.; Eddy, S.R.; Park, Y.; Lopez, R.; Finn, R.D. HMMER web server: 2018 update. *Nucleic Acids Res.* **2018**, *46*, W200–W204.
39. Katoh, K.; Standley, D.M. MAFFT multiple sequence alignment software version 7: improvements in performance and usability. *Mol. Biol. Evol.* **2013**, *30*, 772–780.
40. Minh, B.Q.; Schmidt, H.A.; Chernomor, O.; Schrempf, D.; Woodhams, M.D.; Von Haeseler, A.; Lanfear, R. IQ-TREE 2: new models and efficient methods for phylogenetic inference in the genomic era. *Mol. Biol. Evol.* **2020**, *37*, 1530–1534.
41. Gupta, R.; Brunak, S. Prediction of glycosylation across the human proteome and the correlation to protein function. In *Biocomputing 2002*, 2001; pp. 310–322.
42. DuBois, R.M.; Freiden, P.; Marvin, S.; Reddivari, M.; Heath, R.J.; White, S.W.; Schultz-Cherry, S. Crystal Structure of the Avian Astrovirus Capsid Spike. *J. Virol.* **2013**, *86*, 7853–7863.

 doi:10.20944/preprints202502.0024.v1

43. Waterhouse, A.; Bertoni, M.; Bienert, S.; Studer, G.; Tauriello, G.; Gumienny, R.; Heer, F.T.; de Beer, T.A.P.; Rempfer, C.; Bordoli, L.; Lepore, R. SWISS-MODEL: homology modelling of protein structures and complexes. *Nucleic Acids Res.* **2018**, *46*, W296–W303.
44. Studer, G.; Rempfer, C.; Waterhouse, A.M.; Gumienny, R.; Haas, J.; Schwede, T. QMEANDisCo—distance constraints applied on model quality estimation. *Bioinformatics* **2020**, *36*, 1765–1771.
45. Todd, D.; Trudgett, J.; Smyth, V.J.; Donnelly, B.; McBride, N.; Welsh, M.D. Capsid protein sequence diversity of avian nephritis virus. *Avian Pathol.* **2011**, *40*, 249–259.
46. Espinoza, L.L.; Beserra, L.A.; Soares, R.M.; Gregori, F. Avian nephritis virus (ANV) on Brazilian chickens farms: circulating genotypes and intra-genotypic diversity. *Arch. Virol.* **2016**, *161*, 3455–3462.
47. Kelly, A.G.; Netzler, N.E.; White, P.A. Ancient recombination events and the origins of hepatitis E virus. *BMC Evol. Biol.* **2016**, *16*, 1–18.
48. Pankovics, P.; Boros, Á.; Kiss, T.; Engelmann, P.; Reuter, G. Genetically highly divergent RNA virus with astrovirus-like (5′-end) and hepevirus-like (3′-end) genome organization in carnivorous birds, European roller (Coracias garrulus). *Infect. Genet. Evol.* **2019**, *71*, 215–223.
49. Guy, J.S. Virus infections of the gastrointestinal tract of poultry. *Poult. Sci.* **1998**, *77*, 1166–1175.
50. Lu, J.; Yang, S.; Wang, C.; Wang, H.; Gong, G.; Xi, Y.; Pan, J.; Wang, X.; Zeng, J.; Zhang, J.; Li, P. Gut virome of the world's highest-elevation lizard species (Phrynocephalus erythrurus and Phrynocephalus theobaldi) reveals versatile commensal viruses. *Microbiol. Spectrum* **2022**, *10*, e01872–21.
51. Pantin-Jackwood, M.; Todd, D.; Koci, M.D. Avian astroviruses. In *Astrovirus Research: Essential Ideas, Everyday Impacts, Future Directions*, 2013; pp. 151–180.
52. De Battisti, C.; Salviato, A.; Jonassen, C.M.; Toffan, A.; Capua, I.; Cattoli, G. Genetic characterization of astroviruses detected in guinea fowl (Numida meleagris) reveals a distinct genotype and suggests cross-species transmission between turkey and guinea fowl. *Arch. Virol.* **2012**, *157*, 1329–1337.
53. Chu, D.K.W.; Leung, C.Y.H.; Perera, H.K.K.; Ng, E.M.; Gilbert, M.; Joyner, P.H.; Grioni, A.; Ades, G.; Guan, Y.; Peiris, J.S.M.; Poon, L.L.M. A Novel Group of Avian Astroviruses in Wild Aquatic Birds. *J. Virol.* **2012**, *86*, 13772–13778.
54. Vigerust, D.J.; Shepherd, V.L. Virus glycosylation: role in virulence and immune interactions. *Trends Microbiol.* **2007**, *15*, 211–218.
55. Wickramasinghe, I.A.; De Vries, R.P.; Gröne, A.; De Haan, C.A.M.; Verheije, M.H. Binding of avian coronavirus spike proteins to host factors reflects virus tropism and pathogenicity. *J. Virol.* **2011**, *85*, 8903–8912.
56. Abdelwhab, E.S.M.; Veits, J.; Tauscher, K.; Ziller, M.; Grund, C.; Hassan, M.K.; Shaheen, M.; Harder, T.C.; Teifke, J.; Stech, J.; Mettenleiter, T.C. Progressive glycosylation of the haemagglutinin of avian influenza H5N1 modulates virus replication, virulence and chicken-to-chicken transmission without significant impact on antigenic drift. *J. Gen. Virol.* **2016**, *97*, 3193–3204.
57. Zheng, J.; Yamada, Y.; Fung, T.S.; Huang, M.; Chia, R.; Liu, D.X. Identification of N-linked glycosylation sites in the spike protein and their functional impact on the replication and infectivity of coronavirus infectious bronchitis virus in cell culture. *Virology* **2018**, *513*, 65–74.
58. Dong, J.; Dong, L.; Méndez, E.; Tao, Y. Crystal structure of the human astrovirus capsid spike. *Proc. Natl. Acad. Sci.* **2011**, *108*, 12681–12686.
59. Arias, C.F.; DuBois, R.M. The astrovirus capsid: a review. *Viruses* **2017**, *9*, 15.
60. Bogdanoff, W.A.; Campos, J.; Perez, E.I.; Yin, L.; Alexander, D.L.; DuBois, R.M. Structure of a human astrovirus capsid-antibody complex and mechanistic insights into virus neutralization. *J. Virol.* **2017**, *91*, 10–1128.
61. Bosch, A.; Pintó, R.M.; Guix, S. Human astroviruses. *Clin. Microbiol. Rev.* **2014**, *27*, 1048–1074.
62. Johnson, C.; Hargest, V.; Cortez, V.; Meliopoulos, V.A.; Schultz-Cherry, S. Astrovirus pathogenesis. *Viruses* **2017**, *9*, 22.
63. Thouvenelle, M.L.; Haynes, J.S.; Reynolds, D.L. Astrovirus infection in hatchling turkeys: histologic, morphometric, and ultrastructural findings. *Avian Dis.* **1995**, 328–336.

 doi:10.20944/preprints202502.0024.v1

64. De Wit, J.J.; Dam, G.T.; de Laar, J.V.; Biermann, Y.; Verstegen, I.; Edens, F.; Schrier, C.C. Detection and characterization of a new astrovirus in chicken and turkeys with enteric and locomotion disorders. *Avian Pathol.* **2011**, *40*, 453–461.
65. Saif, Y.M.; Guy, J.S.; Day, J.M.; Cattoli, G.; Hayhow, C.S. Viral enteric infections. *Dis. Poult.* **2020**, 401-445.
66. Li, Y.; Luo, J.; Shang, J.; Zhang, F.; Deng, C.; Feng, Y.; Meng, G.; Jiang, W.; Yu, X.; Liu, H. Epidemiological investigation and pathogenicity analysis of waterfowl astroviruses in some areas of China. *Front. Microbiol.* **2024**, *15*, 1375826.
67. Brown, J.R.; Morfopoulou, S.; Hubb, J.; Emmett, W.A.; Ip, W.; Shah, D.; Brooks, T.; Paine, S.M.; Anderson, G.; Virasami, A.; Tong, C.W. Astrovirus VA1/HMO-C: an increasingly recognized neurotropic pathogen in immunocompromised patients. *Clin. Infect. Dis.* **2015**, *60*, 881–888.
68. Anderson, G.L.; Braun, E.J. Postrenal modification of urine in birds. *Am. J. Physiol. Regul. Integr. Comp. Physiol.* **1985**, *248*, R93–R98.
69. Australian Department of Agriculture, Water and the Environment, Import risk review for psittacine birds from all countries – draft review, Canberra, July 2020. CC BY 4.0. Available online: https://www.agriculture.gov.au/sites/default/files/documents/draft-psittacine-review-for-public-comment.pdf (accessed on 26 August 2024).